# Ambipolar Transport in an Electrochemically Gated Single-Molecule Field-Effect Transistor

**Ismael Díez-Pérez,[†,‡] Zhihai Li,[†] Shaoyin Guo,[†] Christopher Madden,[§] Helin Huang,[⊥] Yanke Che,[⊥] Xiaomei Yang,[⊥] Ling Zang,[*,⊥] and Nongjian Tao[†,*]**

[†]Center for Bioelectronics and Biosensors, Biodesign Institute, Arizona State University, Tempe, Arizona 85287, United States, [‡]Department of Physical Chemistry, University of Barcelona & Institute for Bioengineering of Catalonia (IBEC), Barcelona 08028, Spain, [§]Center for Bioenergy and Photosynthesis, Center for Bio-Inspired Solar Fuel Production, and Department of Chemistry and Biochemistry, Arizona State University, Tempe, Arizona 85287, United States, and [⊥]Department of Materials Science and Engineering, University of Utah, Salt Lake City, Utah 84108, United States

**ABSTRACT**

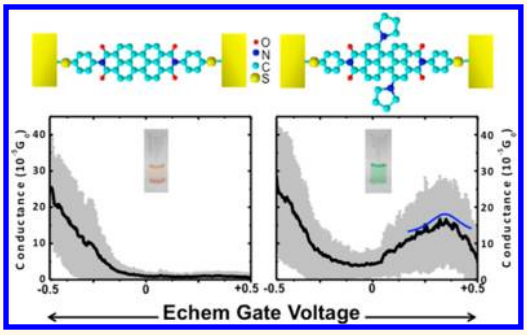


**Charge transport is studied in single-molecule junctions formed with a 1,7-pyrrolidine-substituted 3,4,9,10-perylenetetracarboxylic diimide (PTCDI) molecular block using an electrochemical gate. Compared to an unsubstituted-PTCDI block, spectroscopic and electrochemical measurements indicate a reduction in the highest occupied (HOMO)—lowest unoccupied (LUMO) molecular orbital energy gap associated with the electron donor character of the substituents. The small HOMO—LUMO energy gap allows for switching between electron- and hole-dominated charge transports as a function of gate voltage, thus demonstrating a single-molecule ambipolar field-effect transistor. Both the unsubstituted and substituted molecules display similar n-type behaviors, indicating that they share the same n-type conduction mechanism. However, the substituted-PTCDI block shows a peak in the source—drain current *vs* gate voltage characteristics for the p-type transport, which is attributed to a two-step incoherent transport *via* the HOMO of the molecule.**

**KEYWORDS:** ambipolar FET · single-molecule junction · electrochemical gate · PTCDI · STM

An ambipolar field-effect transistor (FET) is a device that can be switched between n-type and p-type transport behaviors with a gate voltage. Unlike its unipolar counterpart, whose conduction is dominated by one type of charge carrier, electrons or holes, the conduction in the ambipolar FET can be dominated by either electrons or holes, depending on the applied gate voltage. Ambipolar transport behavior was first demonstrated in amorphous Si devices where both charge carriers are provided by trap states in the material.[1] In more recent years, ambipolar conduction has been reported and studied in many postsilicon devices, including carbon nanotubes[2] and graphene,[3] and also in organic crystals[4] and polymers,[5] and more recently in topological insulators.[6] Finally, a few examples of ambipolar single-molecule FET studies at low temperatures can be found.[7,8] The unique ambipolar behavior in molecular devices promises new design principles for both analog and digital applications and new opportunities for one to study both electron- and hole-dominated transport in the same molecule and to understand the role of the HOMO and LUMO in the conduction through the molecule.

Here we report a single-molecule ambipolar FET whose conduction behavior can be reversibly switched between n- and p-types with an electrochemical gate at room temperature. The use of an electrochemical gate provides much more efficiency in the conductance gating of the molecular transistor compared to the more traditional low-temperature solid-state gating. It also opens the door to study various electrochemical behaviors of molecules and to relate the charge transport to the electron transfer (ET) theories developed for solution phase chemistry. In order to achieve an ambipolar effect in a single-molecule junction, molecules with a low HOMO—LUMO energy gap are required.[9,10] In this work, a pyrrolidine-substituted perylenetetracarboxylic diimide (PTCDI) derivative with a low HOMO—LUMO energy gap is

* Address correspondence to njtao@asu.edu; lzang@eng.utah.edu.

Received for review May 11, 2012 and accepted July 12, 2012.

**Published online** 10.1021/nn302090t

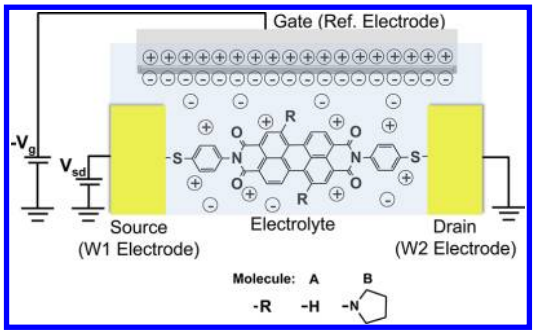


**Figure 1. Schematic experimental setup of the single-molecule FETs measured in this work. W1 (source) and W2 (drain) electrodes are the Au surface and STM tip electrodes, respectively, in the employed STM configuration. Molecules A and B correspond to the unsubstituted and pyrrolidine-substituted PTCDI blocks, respectively.**

synthesized and bridged between two gold electrodes using thiolated terminal groups. The Fermi energy levels of the gold electrodes lie within the HOMO–LUMO energy gap of the molecule close to both HOMO and LUMO energy levels. By changing the gate voltage, we move the Fermi levels toward the HOMO or LUMO levels, leading to p- or n-type conductions, respectively. As a control experiment, an unsubstituted PTCDI derivative is also studied, which exhibits n-type behavior only. The observations are consistent with optical spectroscopy, electrochemical data, and density functional theory (DFT) calculations of both unsubstituted and substituted PTCDI molecules, further supporting the interpretation of the ambipolar character of the charge transport in the pyrrolidine-substituted PTCDI junction. In addition, we show that the n-type transport in the substituted molecule is similar to that in the unsubstituted molecule, while the p-type transport in the substituted one can be described by an adiabatic two-step ET process.

## RESULTS AND DISCUSSION

**Electrochemically Gated Single-PTCDI Junctions.** The experimental setup is represented in Figure 1. A PTCDI molecule is bridged between two gold electrodes (source and drain) to form a molecular junction immersed in an electrolyte, and the charge transport through the junction is controlled with an electrochemical gate electrode immersed in the same electrolyte. This electrochemical gating method is more efficient than the traditional solid-state gating[6,7,11,12] and has been previously employed to demonstrate FET behavior in single-molecule junctions.[13–15] Two molecules are studied in this work, a 1,7-pyrrolidine-substituted PTCDI and an unsubstituted analogue (see Supporting Information (SI) for details on the synthesis). The latter served as a control. Both molecules contain two mercaptophenyl groups at the N-imide positions on both sides of the molecule that served both as covalent anchoring (through thiol–gold bonding) and electronic coupling between the molecule and the two gold electrodes.[16,17]

**Optical Spectroscopy, Electrochemical, and DFT Data.** The optical spectra of the two molecules show that the pyrrolidine substitution in the PTCDI block causes a strong optical red shift in the absorption spectrum (Figure 2a), which indicates a smaller HOMO–LUMO energy gap.[18,19] The red shift is also consistent with previously reported works on redox-active chromophores with pyrrolidine substitutions.[20] DFT calculations further confirm the reduction of the HOMO–LUMO energy gap (see SI Figure S1).

The optical absorption data provide useful information about the HOMO–LUMO energy separation, but they do not tell us about the alignment of the HOMO and LUMO energy levels of the molecule relative to the Fermi energy levels of the gold electrodes. To access this information, we carried out electrochemical measurements of the molecules adsorbed on gold electrodes. Due to the relatively low coverage of the molecules on the gold electrode surface, we used differential pulse voltammetry, which suppresses background polarization current and helps to resolve the peaks in the voltammogram due to the molecular redox processes. As shown in Figure 2b, the anodic (HOMO-related) redox peak (with a smaller shoulder) of the pyrrolidine-substituted PTCDI has a cathodic shift of ~0.6 V relative to that of the unsubstituted PTCDI. This observation suggests that the pyrrolidine substitution not only reduces the HOMO–LUMO energy gap separation, but also results in a better alignment of the HOMO level with the gold electrode Fermi energy. To support the differential pulse voltammetry data, we also carried out standard electrochemical measurements on the pyrrolidine-substituted and unsubstituted PTCDIs dissolved in an electrolyte rather than adsorbed on the electrode surface (Figure S2a and b). While the voltammetry of the substituted compound (Figure S2b) was able to clearly resolve both LUMO- and HOMO-related redox processes, showing good agreement with the HOMO peak position of Figure 2b, the poor resolution of the redox processes for the unsubstituted molecule was the result of the encountered solubility issues and strong aggregation character of this compound through, most likely, $\pi-\pi$ stacking, which obscured the electron exchange between the molecules in solution and the electrode surface. Although the trend of the HOMO-related peak is the same as in Figure 2b between the two compounds, its position in Figure S2a is purely qualitative.

Summing up, the electrochemical data on the absorbed molecules shown in Figure 2b are a reliable way to compare the effect of the pyrrolidine substitution on the HOMO-related redox processes and a good platform to compare the electrochemical activity to the single-molecule transport measurements where the molecules are absorbed between two electrodes. Together with the optical absorption spectra, these data

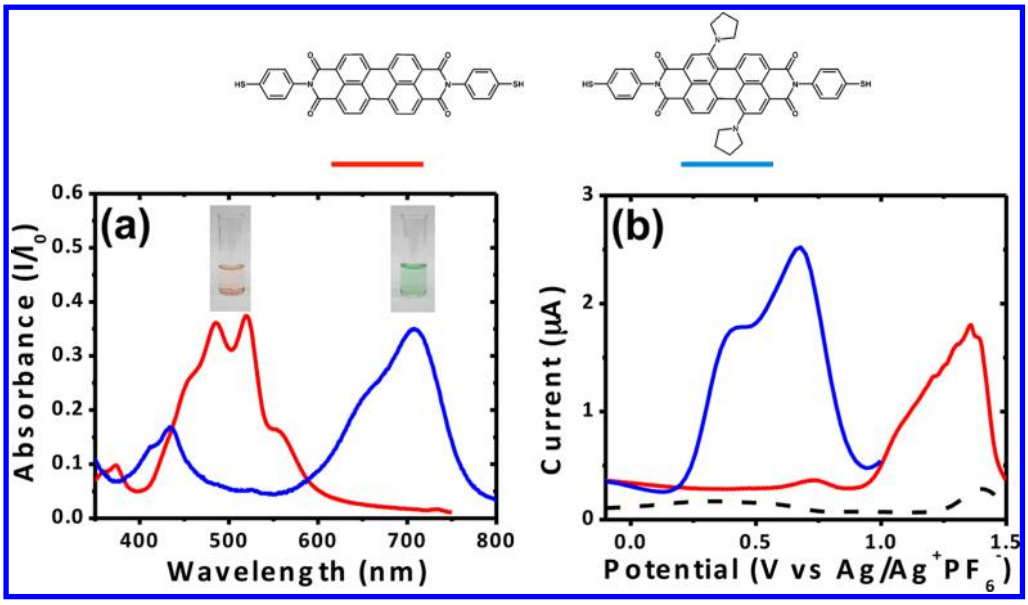


**Figure 2. UV−visible spectra (a) and differential pulse voltammograms of a Au electrode surface modified with the target molecules (b) for the unsubstituted PTCDI (red curves) and the pyrrolidine-substituted PTCDI (blue curves). All measurements were performed in acetonitrile with 20 mM tetrabutylammonium hexafluorophosphate ($TBAPF_6$) as the electrolyte. The inset in (a) shows photos of acetonitrile solutions of the two molecules. The electrochemical pulse parameters in (b) were 0.5 s interval time and 30 mV amplitude.**

strongly support the interpretation of the transport data, as will be shown below.

**Conductance of the Single-Molecule Junctions.** We measured the conductance of single-molecule junctions of the pyrrolidine-substituted and unsubstituted PTCDI molecules using a scanning tunneling microscope (STM) break junction method.[21] Details of the experimental procedure can be found in the Methods section. Briefly, an Apiezon-coated Au STM tip was brought into contact with a gold substrate electrode covered with the target molecule, during which the current between the tip and substrate electrodes under a fixed bias voltage ($V_{bias}$) was continuously monitored. Once the current reached a preset value, the STM tip was retracted until it dropped to a lower current set point value. The process was then repeated, and a large number of current/conductance traces were recorded during the retraction stage.

Figure 3a and b plot typical individual current/conductance traces for the unsubstituted and pyrrolidine-substituted PTCDI molecules, respectively. Each trace displays a step-like feature, which is attributed to the formation of a single-molecule junction.[21] About 40% of the total recorded individual traces showed such a step-like feature. Within the traces displaying a step-like feature, about half of them showed rather flat steps (*e.g.*, black curves in Figure 3a and b), while the other half clearly showed tilted step features (red curves in Figure 3a). The titled steps have been observed in previous single-molecule junction measurements containing a rigid conjugated backbone such as the perylene blocks used in this study,[22−24] and they have been ascribed to the overlapping between the $\pi$-orbitals of the conjugated molecular block and the orbitals of the two metal electrodes.[25,26] This orbital coupling contributes to a larger conductance of the single-molecule junction, but it decreases as the two electrodes are pulled apart, leading to a gradual decrease in the conductance, which is observed as a tilted step in the conductance *vs* distance traces[22,24] (red curves in Figure 3a). In contrast, the traces with flat steps correspond to the molecular configurations in which the coupling of the $\pi$-orbitals with the electrodes is minimal (*e.g.*, the molecule in the last stage of the pulling is nearly perpendicular to the electrode surface). In this case, the conductance values correspond almost exclusively to the conductance through the molecular backbone.

To avoid ambiguity in determining the conductance of the molecules, we constructed conductance histograms with current traces displaying plateaus with little or no tilting (black curves in Figure 3a and b). Figure 3c and d are the resulting conductance histograms for the unsubstituted and pyrrolidine-substituted PTCDI molecules, respectively, each showing a distinct peak marked by an arrow. The blue lines represent Gaussian fits to the peaks, from which conductance values for both unsubstituted and substituted molecules are determined to be $8.8 \times 10^{-6} G_0$ and $4.5 \times 10^{-5} G_0$, respectively ($G_0 = 77.4\ \mu S$ is the conductance quantum). Control experiments were carried out by following the same sample preparation procedures but in the absence of target molecules. The measured conductance traces in this case did not display clear step-like features, and consequently the conductance histogram shows no peak (gray lines in Figure 3c and d).

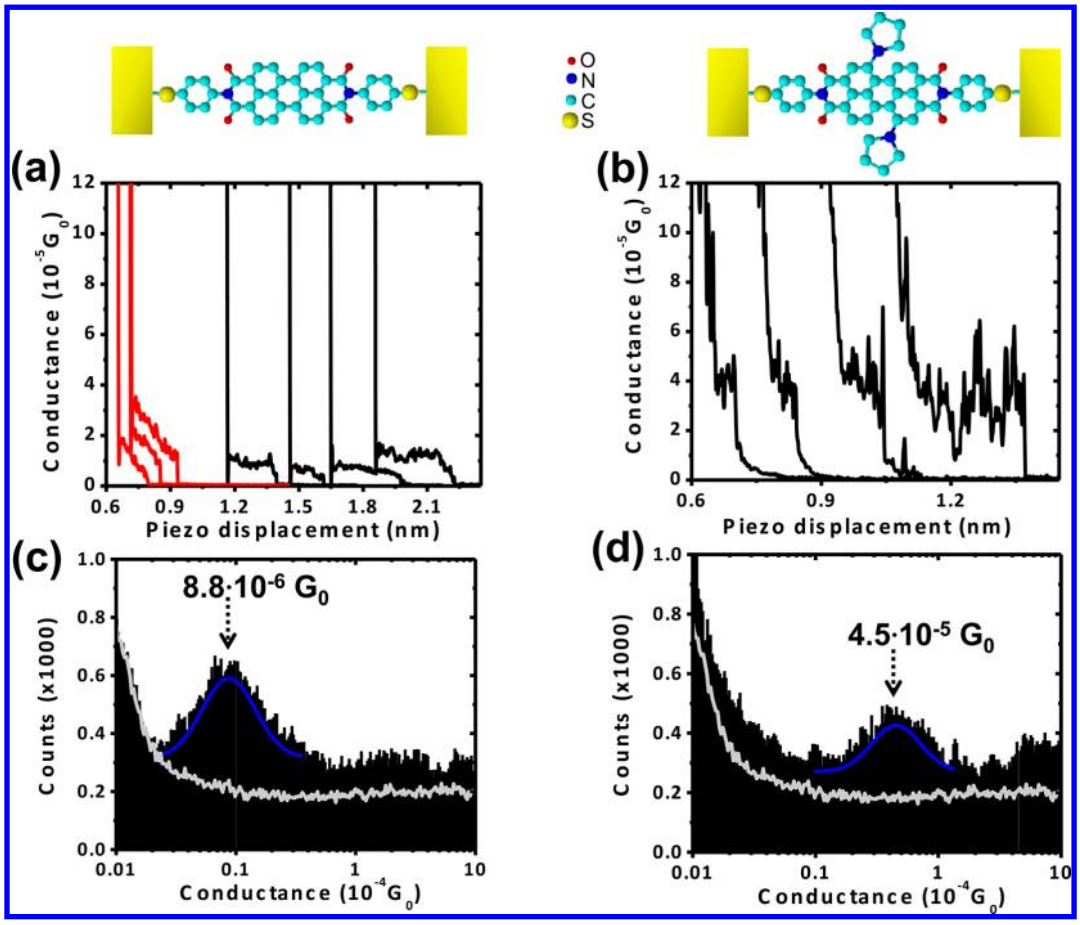


**Figure 3. Single-molecule conductance experiments with the break-junction method: (a, b) Representative pulling traces for the unsubstituted and the pyrrolidine-substituted PTCDI, respectively. Red curves in (a) are typical pulling traces displaying lateral coupling effects (see text for details). (c, d) Conductance histograms built from thousands of black traces in (a) and (b), respectively. The single-molecule conductance values are taken from the Gaussian fits (blue lines) of the most prominent peaks in the histograms. The gray lines are the conductance histogram in the absence of molecules. The electrochemical gate voltage for the W1 electrode was set to 50 mV and the sample $V_{bias}$ to 0.2 V.**

**Single-Molecule Charge Transport Measurement.** To study the electrochemical gate effect on the single-molecule junctions with both molecules, we use a "blinking" method.[27−29] In this method the STM tip electrode was brought close to the substrate electrode on which the sample molecules were adsorbed. The gap separation between the tip and substrate was controlled by the STM feedback loop to the current, which was initially set to a value of less than 20 pA, which roughly corresponds to a tip−substrate separation of ∼2 nm, slightly smaller than the molecular length (∼2.3 nm). The feedback loop was then turned off, and the current was continuously monitored. Once a molecule bridges between the surface and tip electrodes, a large and sudden increase in the junction conductance was observed and an electrochemical gate voltage ramp was triggered to measure the current through the molecule as a function of gate voltage. Figure 4a and b are some of the current *vs* time traces recorded with the "blinking" method, showing sudden jumps in the current from the low initial set point current level to a higher value (left side in Figure 4a and b). The stepwise current increase is due to the formation of a single-molecule bridge, and the conductance determined from the current step matches well with the conductance obtained from the conductance histograms shown in Figure 3. We frequently observed single-molecule junctions that lasted for seconds, which allowed us to determine the charge transport behavior through the molecules by sweeping the electrochemical gate voltage.

Figure 4c and d show several representative curves of the gate-dependent source−drain current for the unsubstituted and pyrrolidine-substituted PTCDIs, respectively. There is a clear junction-to-junction variation in the gate-controlled current, most likely due to structural and contact geometry differences. However, the overall source−drain current *vs* gate voltage curves show distinct reproducible trends for both molecules, as observed in the average source−drain current *vs* electrochemical gate characteristics built out of tens of previous individual traces (Figure 4e and f). Note that the gate voltage range was kept within ±0.6 V because the single-molecule junctions become increasingly unstable outside of this voltage range, causing the breakdown of the junction, which is observed as a sudden drop of the current to a the lower initial set

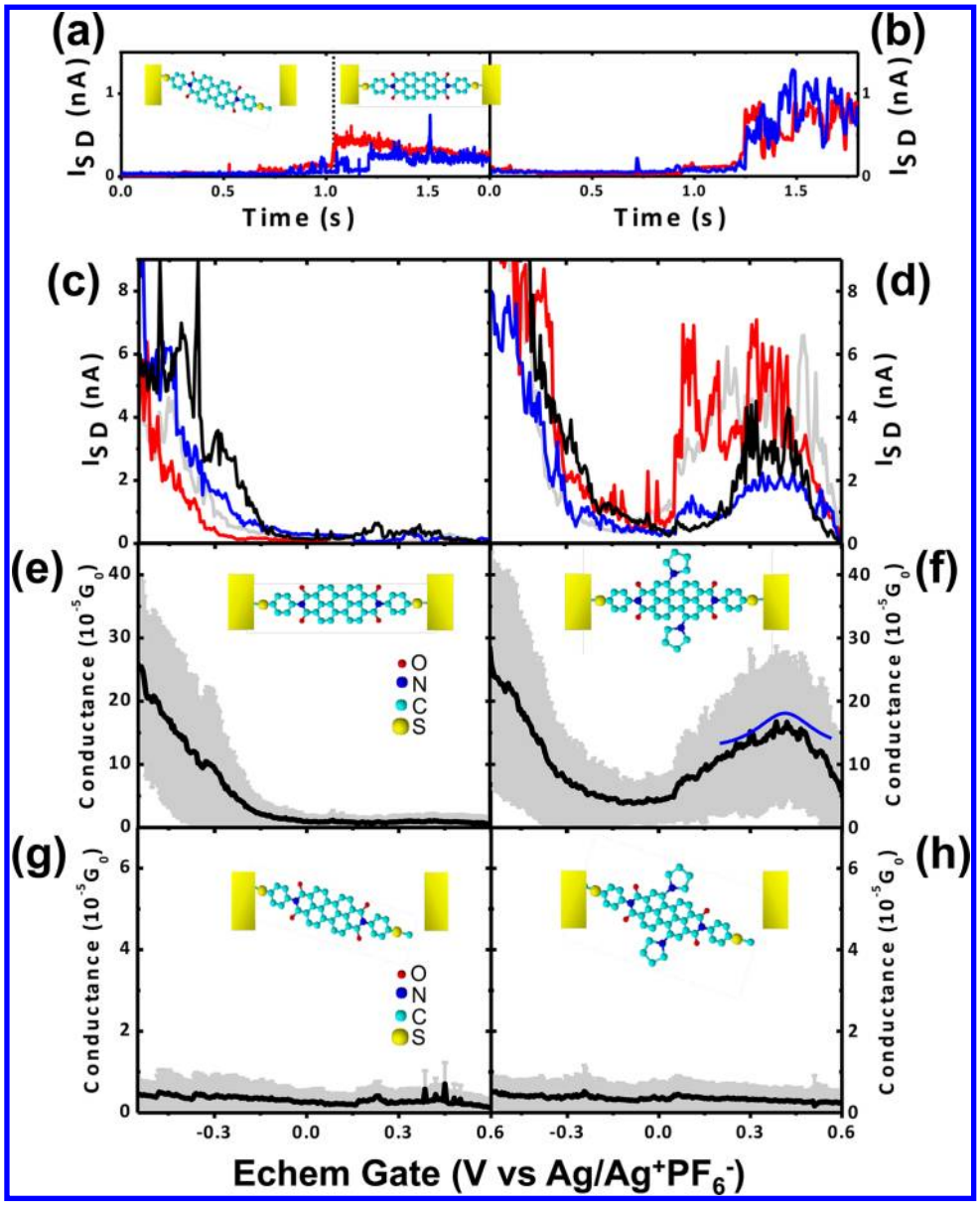


**Figure 4. Single-molecule FET experiments: (a, b) "Blinking" traces showing single-molecule bridging events for the unsubstituted and the pyrrolidine-substituted PTCDI, respectively. Sudden jumps in the dc current (right side of the graphs) mean formation of a single-molecule junction (see insets in (a)). (c, d) Representative source−drain current *vs* electrochemical gate voltage curves of different junctions for the unsubstituted and the pyrrolidine-substituted PTCDI, respectively. Different colors in (a)−(d) represent independent measurements. Negative and positive electrochemical voltages mean LUMO and HOMO transport, respectively. (e, f) Average conductance *vs* electrochemical gate voltage for junctions with the unsubstituted and the pyrrolidine-substituted PTCDI, respectively. The gray shadow corresponds to the standard deviation for $N$ = 75 and 85 for (e) and (f), respectively. The two-step tunneling model (eq 2) is included in (f) with a positive Y-offset for a better visualization (blue curve), and the quantitative model fitting is shown in Figure 5b. (g, h) Control experiments: average conductance *vs* electrochemical gate curves for open junctions in the presence of unsubstituted and pyrrolidine-substituted PTCDI, respectively. Gray shadow in graphs represents the standard deviation for $N$ = 32 in both cases. In all experiments, a constant sample $V_{bias}$ of 0.2 V was applied.**

point value (see an example of a junction breakdown in Figure S3b). We discuss in detail the conductance *vs* gate voltage behavior of the two molecules below.

The single-molecule junctions for the unsubstituted PTCDI block (Figure 4c and e) show a clear n-type FET behavior, in which the current increases as the gate voltage sweeps negatively relative to the reference electrode, corresponding to the approach of the LUMO to the Fermi energy levels of the electrodes and leading to an electron-dominated charge transport. This observation is in good agreement with previous works on the same molecular block carried out in an aqueous electrolyte within a narrower gate voltage range[13,30,31] and confirmed by first-principle calculations.[32] No current increase was observed at positive gate voltages (HOMO-related) in this case. This is also in agreement with the electrochemical data (Figure 2b) that show that the HOMO-related redox peak for the unsubstituted molecule is well above the upper limit of the applied gate voltage.

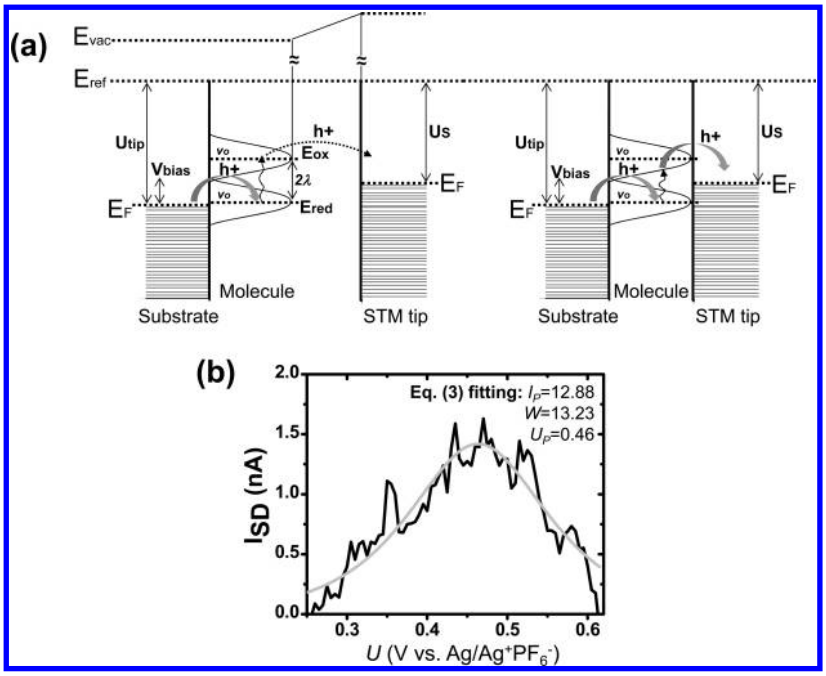


**Figure 5. Two-step ET model: (a) Schematic representation of a two-step ET mechanism in both partially adiabatic limit, representing an STM configuration (left panel), and fully adiabatic limit, representing a single-molecule junction (right panel). (b) Fitting of the average experimental source−drain current *vs* electrochemical voltage curve in Figure 4f (black curve) to the two-step tunneling model (eq 3, gray curve). The inset shows the resulting values for the fitting parameters of the model.**

For the pyrrolidine-substituted PTCDI, the gate dependence in the negative voltages shows a clear n-type FET behavior, which is nearly identical to that of the unsubstituted molecule (Figure 4f), indicating that both molecules share the same n-type conduction mechanism. However, the positive gate voltage sweep also leads to an increase in the current through the pyrrolidine-substituted PTCDI junction, which is in sharp contrast to the behavior of the unsubstituted PTCDI. Because sweeping the gate positively corresponds to shifting the HOMO closer to the electrode Fermi energy levels, the increase in the current with positive sweep of the gate voltage indicates a hole-dominated transport or p-type FET behavior. The results show that the pyrrolidine-substituted PTCDI junctions can be switched from an electron-dominated to a hole-dominated transport mechanism, thus demonstrating that the ambipolar FET behavior can be achieved in a single-molecule junction by tuning the molecular electronic states with chemical substitutions. Further increasing the gate voltage in the positive direction results in a decrease in the current, leading to a broad peak centered at ~0.5 V. The peak position is close to the redox peak position previously observed in the voltammogram (Figure 2b).

To further confirm that the above observations are due to charge transport through the molecules, control experiments were carried out in cases where the molecules are present but not connected to both the STM tip and substrate electrodes (Figure 4g and h for the substituted and unsubstituted molecules, respectively). Such cases correspond to the low-current regime of the "blinking" traces shown in Figure 4a and b (left side of the traces). Very weak or no gate effect was observed in these cases. Further controls of the background noise current as a function of gate voltage are presented in Figure S3a.

The presence of a peak in the current *vs* electrochemical gate curve and its location near the redox potential for the pyrrolidine-substituted PTCDI strongly suggest a two-step tunneling process for the p-type (HOMO) transport of this molecule. The formalism for such a two-step tunneling process has been developed by Kutentzov and Ulstrup[33−35] and applied to different molecular redox systems, mostly for electron transport.[36−39] Here we adopt the formalism for hole transport. As represented in Figure 5a, a hole first tunnels from the left electrode to the molecule, and the molecule and its surrounding environment relax either fully (left panel) or partially (right panel), depending on the coupling strengths between the molecule and the two electrodes. These two scenarios have been referred to as diabatic and adiabatic limits, respectively. The hole loses coherence during the relaxation process. In a second step, the hole tunnels from the molecule to the right electrode. The total current *via* the two-step tunneling process is given by[34,35]

$$I = A\frac{K_{LM}K_{MR}}{K_{LM} + K_{MR}} \quad (1)$$

which was derived from the rate equation of two sequential and independent electron transfer steps,[40] where $k_{LM}$ and $k_{MR}$ represent rate constants ($s^{-1}$) of the ET from the Au substrate electrode to the molecule and from the molecule to the STM tip, respectively. In eq 1, $A$ is a parameter that take two different forms depending on

whether the process is closer to the diabatic or adiabatic limits, but the shape of the current *vs* gate voltage characteristic is determined by the rate constants $k$, which depend on the bias voltage ($V_{bias}$) between the two electrodes (source and drain), the overpotential ($\eta = U - U^0$, the gate voltage with respect to the standard redox potential $U^0$), the reorganization energy ($\lambda$), *etc.*[41,42] Wandlowski *et al.*[37] have obtained a simplified expression for the total current $I$ (in nA) by assuming the fully adiabatic limit (strong coupling between both molecule and electrodes) and approximating to low $\eta$ and $V_{bias}$:

$$I = \frac{910V_{bias}\exp[-9.73(\lambda + V_{bias})]}{\cosh[19.4\left(\xi\eta + \left(\gamma - \frac{1}{2}\right)V_{bias}\right)]} \quad (2)$$

where $\xi$ and $\gamma$ are model parameters, ranging between 0 and 1, describing the effective applied gate and bias voltages, respectively, at the location of the redox center of the molecule. Equation 2 can be rearranged as

$$I = \frac{I_P}{\cosh[W(U - U_P)]} \quad (3)$$

which predicts a peak in the current *vs* gate voltage curve with position $U_P$ and height $I_P$ described as

$$U_P = U^0 + \frac{(0.5 - \gamma)V_{bias}}{\xi} \quad (4)$$

$$I_P = 910V_{bias}\exp[-9.73(\lambda + V_{bias})] \quad (5)$$

and width described by the model parameter $W$:

$$W = 19.4\xi \quad (6)$$

where a higher $W$ value means a narrower peak.

We fit the average experimental source–drain current *vs* electrochemical gate voltage curve to eq 3 (Figure 5b), resulting in the fitting parameters $I_P$ =12.88 nA, $U_P$ =0.46 V, and $W$ = 13.23. From the $I_P$ value and using eq 5, we obtained a reorganization energy value of $\lambda = 0.3 \pm 0.05$ eV, which is consistent with previously reported values for other rigid conjugated redox molecules[37] and model redox proteins.[38,39] From the $W$ value and using eq 6, we also get $\xi$ = 0.66, which suggests a partial screening of the applied overpotential at the redox center. There is strong correlation between the model parameters $U^0$ and $\gamma$. Because the junction is symmetric (at least on average based on the symmetry of the molecule), we fixed $\gamma$ to 0.5 and then get $U_0$ = 0.46 V through eq 4, which is somewhat smaller than the $U_{1/2}$ value (0.55 V) obtained from the cyclic voltammogram (Figure S2b). The small discrepancy may be attributed to the difference between the single-molecule junction measurement, where the molecule is sandwiched between two electrodes, and the cyclic voltammogram, where the molecules are absorbed on one electrode surface only. This explanation is consistent with the observed partial screening of the redox center ($\xi$ < 1) by the proximity of the two electrodes. We conclude here that the good-fitting results and the reasonable $\lambda$ obtained values indicate that the two-step tunneling model provides a plausible explanation for the p-type transport behavior in the pyrrolidine-substituted PTCDI junction.

## CONCLUSIONS

In summary, we have demonstrated room-temperature ambipolar FET behavior in a single-molecule junction by studying charge transport in two structurally related molecules, an unsubstituted PTCDI and a pyrrolidine-substituted PTCDI block. Optical absorption spectroscopy, electrochemical measurements, and DFT calculations show that the introduction of the pyrrolidine groups to the conjugated PTCDI backbone results in a decrease of the molecular HOMO–LUMO energy gap and a shift of the HOMO level closer to the electrodes' Fermi energy levels. Using an electrochemical voltage gating method, we are able to bring either the LUMO or HOMO of the pyrrolidine-substituted PTCDI molecule close to the Fermi energy levels of the electrodes and to switch the charge transport behavior from electron-dominated to hole-dominated, leading to ambipolar behavior in a single-molecule FET. Furthermore, a peak is observed in the p-type regime of the conductance *vs* gate characteristic, which is attributed to an adiabatic two-step tunneling process. This model has been previously demonstrated to be useful for describing electron-dominated transport through single-molecule junctions with redox activity, and it is shown here to provide also a reasonable description for hole-dominated transport. The narrow HOMO–LUMO gap of the pyrrolidine-substituted PTCDI derivative allows easy switching between hole- and electron-dominated charge transport regimes through an electrochemical gate voltage, making them attractive for studying the fundamental redox properties of single molecules and for the prospect of future applications on organic electrical devices where the transport regime could be easily tuned *via* a small applied gate voltage.

## METHODS

**Optical Spectroscopy and Electrochemical Measurements.** Optical spectra were recorded from $\mu$M solutions of both PTCDI molecules in benzonitrile/20 mM $TBAPF_6$. Differential pulse voltammetry was performed to characterize the redox activity of the PTCDI molecules adsorbed on Au electrodes. The PTCDI-modified electrode surfaces were prepared by immersing freshly prepared Au substrates (see below for details on Au surface preparation) in $\mu$M benzonitrile solutions of the target molecules for several hours (<12 h). The Au electrodes covered with the molecules were then washed thoroughly with benzonitrile,

acetonitrile, and ethanol, successively. The electrodes were then dried under an Ar atmosphere and then transferred to the electrochemical cell. We used a conventional three-electrode electrochemical cell using a Pt coil as the counter electrode and a Ag wire as the reference electrode. As the working electrolyte, we used 20 mM tetrabutylammonium hexafluorophosphate ($TBAPF_6$) dissolved in acetonitrile (MeCN) (both analytical grade from Sigma-Aldrich) in all cases, except for the standard cyclic voltammetry of Figure S2, where benzonitrile was used instead. Other than the cyclic voltammograms represented in Figure S2, all electrochemical potentials or gate voltages in this work are quoted *vs* a Ag wire ($Ag/Ag^+PF_6^-$ in this particular electrolyte), which is a widely used quasi-reference electrode in STM experiments.

**STM Break-Junction Measurements.** The STM break-junction method was conducted with a Molecular Imaging STM (Agilent, USA) controlled by a Nanoscope E (Bruker, USA). In the break-junction experiment, a 2-point feedback system (maximum and minimum set point currents) is used to control the STM tip position. The STM tip was first moved to the electrode surface until a maximum set point current, typically ranging from 10 to 100 nA (for 1 to 10 nA/V current amplifications respectively), is reached. Then, the tip is retracted until a minimum set point current, typically of ~10 pA, is achieved. The process was typically repeated ~3000 times to obtain a large number of current *vs* time traces, which are transformed into current *vs* piezo displacement (or tip−electrode separation in nm) by using the piezo sensitivity value (in nm/V) and the applied piezo driver scan rate (in V/s). Several examples of such traces are presented in Figure 3a, b. About 500 of these traces displayed flat step-like features, which are used to build conductance histograms (Figure 3c, d).

The break-junction experiments were conducted in 20 mM $TBAPF_6$ dissolved in acetonitrile (MeCN) (both analytical grade from Sigma-Aldrich). The STM tips were made by mechanically cutting a 0.25 mm 99.99% Au wire (Alfa Aesar, USA) and were coated with Apiezon wax so that the leakage current was less than 10 pA. The Au electrode surfaces were prepared by thermally evaporating ~130 nm gold (99.999%, Alfa Aesar) on a freshly cleaved mica slide (Ted Pella) in a UHV chamber at $5 \times 10^{-8}$ Torr. Before each measurement, the Au electrode surface was annealed in a hydrogen flame briefly to remove contamination and to form an atomically flat surface. The electrochemical gate voltage was applied through a bipotentiostat (Agilent) with an applied relatively small bias voltage (0.05−0.2 V) between the STM tip and substrate electrodes.

*Conflict of Interest:* The authors declare no competing financial interest.

*Acknowledgment.* The work is supported by National Science Foundation (CHE-1105588, CHE-0931466, and ECS-0925498). I.D.-P. thanks the Ramon y Cajal program from the Spanish Ministry of Economy and Competitiveness and the EU International Reintegration Grant (FP7-PEOPLE-2010-RG-277182) for financial support.

*Supporting Information Available:* Technical details on the DFT calculations, synthetic route for the substituted PTCDI block, and additional voltammetry of the molecules in solution as well as additional control experiments for the single-molecule transport measurements. This material is available free of charge *via* the Internet at http://pubs.acs.org.

## REFERENCES AND NOTES

1. Matsumura, M.; Nara, Y. High-Performance Amorphous-Silicon Field-Effect Transistors. *J. Appl. Phys.* **1980**, *51*, 6443–6444.
2. Heinze, S.; Radosavljević, M.; Tersoff, J.; Avouris, Ph. Unexpected Scaling of the Performance of Carbon Nanotube Schottky-Barrier Transistors. *Phys. Rev. B* **2003**, *68*, 235418.
3. Novoselov, K. S.; Geim, A. K.; Morozov, S. V.; Jiang, D.; Zhang, Y.; Dubonos, S. V.; Grigorieva, I. V.; Firsov, A. A. Electric Field Effect in Atomically Thin Carbon Films. *Science* **2004**, *306*, 666–669.
4. Dodabalapur, A.; Katz, H. E.; Torsi, L.; Haddon, R. C. Organic Heterostructure Field-Effect Transistors. *Science* **1995**, *269*, 1560–1562.
5. Yuen, J. D.; Fan, J.; Seifter, J.; Lim, B.; Hufschmid, R.; Heeger, A. J.; Wudl, F. High Performance Weak Donor−Acceptor Polymers in Thin Film Transistors: Effect of the Acceptor on Electronic Properties, Ambipolar Conductivity, Mobility, and Thermal Stability. *J. Am. Chem. Soc.* **2011**, *133*, 20799–20807.
6. Yuan, H.; Liu, H.; Shimotani, H.; Guo, H.; Chen, M.; Xue, Q.; Iwasa, Y. Liquid-Gated Ambipolar Transport in Ultrathin Films of a Topological Insulator $Bi_2Te_3$. *Nano Lett.* **2011**, *11*, 2601–2605.
7. Kubatkin, S.; Danilov, A.; Hjort, M.; Cornil, J.; Bredas, J.-L.; Stuhr-Hansen, N.; Hedegard, P.; Bjørnholm, T. Single-Electron Transistor of a Single Organic Molecule with Access to Several Redox States. *Nature* **2003**, *425*, 698–701.
8. Kervennic, Y.-V.; Thijssen, J. M.; Vanmaekelbergh, D.; Dabirian, R.; Jenneskens, L. W.; van Walree, C. A.; van der Zant, H. S. J. Charge Transport in Three-Terminal Molecular Junctions Incorporating Sulfur-End-Functionalized Tercyclohexylidene Spacers. *Angew. Chem., Int. Ed.* **2006**, *118*, 2602–2604.
9. Chikamatsu, M.; Mikami, T.; Chisaka, J.; Yoshida, Y.; Azumi, R.; Yase, K.; Shimizu, A.; Kubo, T.; Morita, Y.; Nakasuji, K. Ambipolar Organic Field-Effect Transistors Based on a Low Band Gap Semiconductor with Balanced Hole and Electron Mobilities. *Appl. Phys. Lett.* **2007**, *91*, 043506.
10. Ye, Q.; Chang, J.; Huang, K.-W.; Chi, C. Thiophene-Fused Tetracene Diimide with Low Band Gap and Ambipolar Behavior. *Org. Lett.* **2011**, *13*, 5960–5963.
11. Ye, J. T.; Inoue, S.; Kobayashi, K.; Kasahara, Y.; Yuan, H. T.; Shimotani, H.; Iwasa, Y. Liquid-Gated Interface Superconductivity on an Atomically Flat Film. *Nat. Mater.* **2010**, *9*, 125–128.
12. White, H. S.; Kittlesen, G. P.; Wrighton, M. S. Chemical Derivatization of an Array of Three Gold Microelectrodes with Polypyrrole: Fabrication of a Molecule-Based Transistor. *J. Am. Chem. Soc.* **1984**, *106*, 5375–5377.
13. Li, C.; Mishchenko, A.; Li, Z.; Pobelov, I.; Wandlowski, T.; Li, X. Q.; Wurthner, F.; Bagrets, A.; Evers., F. Electrochemical Gate-Controlled Electron Transport of Redox-Active Single Perylene Bisimide Molecular Junctions. *J. Phys.: Condens. Matter* **2008**, *20*, 374122.
14. Xiao, X. Y.; Nagahara, L. A.; Rawlett, A.; Tao, N. J. Electrochemical Gate Controlled Conductance of Single Oligo(phenylene ethynylene)s. *J. Am. Chem. Soc.* **2005**, *127*, 9235–9240.
15. He, J.; Fu, Q.; Lindsay, S.; Ciszek, J. W.; Tour, J. M. The Electrochemical Origin of Voltage Controlled Molecule Conductance Switching. *J. Am. Chem. Soc.* **2006**, *128*, 14828–14835.
16. Li, X. L.; He, J.; Hihath, J.; Xu, B. Q.; Lindsay, S. M.; Tao, N. J. Conductance of Single Alkanedithiols: Conduction Mechanism and Effect of Molecule-Electrode Contacts. *J. Am. Chem. Soc.* **2006**, *128*, 2135–2141.
17. Díez-Pérez, I.; Li, Z.; Hihath, J.; Li, J.; Zhang, C.; Yang, X.; Zang, L.; Dai, Y.; Feng, X.; Muellen, K.; *et al*. Gate-Controlled Electron Transport in Coronenes as a Bottom-up Approach towards Graphene Transistors. *Nat. Commun.* **2010**, *1*, 31.
18. Katsuta, S.; Miyagi, D.; Yamada, H.; Okujima, T.; Mori, S.; Nakayama, K.; Uno, H. Synthesis, Properties, and Ambipolar Organic Field-Effect Transistor Performances of Symmetrically Cyanated Pentacene and Naphthacene as Air-Stable Acene Derivatives. *Org. Lett.* **2011**, *13*, 1454–1457.
19. Liu, C.; Liu, Z.; Lemke, H. T.; Tsao, H. N.; Naber, R. C. G.; Li, Y.; Banger, K.; Mullen, K.; Nielsen, M. M.; Sirringhaus, H. High-Performance Solution-Deposited Ambipolar Organic Transistors Based on Terrylene Diimides. *Chem. Mater.* **2010**, *22*, 2120–2124.
20. Martineau, D.; Beley, M.; Gros, P. C. Pyrrolidine-Containing Polypyridines: New Ligands for Improved Visible Light Absorption by Ruthenium Complexes. *J. Org. Chem.* **2006**, *71*, 566–571.
21. Xu, B.; Tao, N. J. Measurement of Single-Molecule Resistance by Repeated Formation of Molecular Junctions. *Science* **2003**, *301*, 1221–1223.

22. Diez-Perez, I.; Hihath, J.; Hines, T.; Wang, Z.-S.; Zhou, G.; Müllen, K.; Tao, N. J. Controlling Single-Molecule Conductance through Lateral Coupling of Pi Orbitals. *Nat. Nanotechnol.* **2011**, *6*, 226–231.
23. Meisner, J. S.; Kamenetska, M.; Krikorian, M.; Steigerwald, M. L.; Venkataraman, L.; Nuckolls, C. A Single-Molecule Potentiometer. *Nano Lett.* **2011**, *11*, 1575–1579.
24. Perrin, M. L.; Prins, F.; Martin, C. A.; Shaikh, A. J.; Eelkema, R.; van Esch, J. H.; Briza, T.; Kaplanek, R.; Kral, V.; van Ruitenbeek, J. M.; *et al*. Influence of the Chemical Structure on the Stability and Conductance of Porphyrin Single-Molecule Junctions. *Angew. Chem., Int. Ed.* **2011**, *50*, 11223–11226.
25. Kornilovitch, P. E.; Bratkovsky, A. M. Orientational Dependence of Current Through Molecular Films. *Phys. Rev. B* **2001**, *64*, 195413.
26. Bratkovsky, A. M.; Kornilovitch, P. E. Effects of Gating and Contact Geometry on Current through Conjugated Molecules Covalently Bonded to Electrodes. *Phys. Rev. B* **2003**, *67*, 115307.
27. Haiss, W.; Nichols, R. J.; van Zalinge, H.; Higgins, S. J.; Bethell, D.; Schiffrin, D. J. Measurement of Single Molecule Conductivity Using the Spontaneous Formation of Molecular Wires. *Phys. Chem. Chem. Phys.* **2004**, *6*, 4330–4337.
28. Chang, S.; He, J.; Kibel, A.; Lee, M.; Sankey, O. F.; Zhang, P.; Lindsay, S. M. Tunneling Readout of Hydrogen-Bonding Based Recognition. *Nat. Nanotechnol.* **2009**, *4*, 297–301.
29. Díez-Pérez, I.; Hihath, J.; Lee, Y.; Yu, L.; Adamska, L.; Kozhushner, M. A.; Oleynik, I. I.; Tao, N. J. Rectification and Stability of a Single Molecular Diode with Controlled Orientation. *Nat. Chem.* **2009**, *1*, 635–641.
30. Xu, B.; Xiao, X.; Yang, X.; Zang, L.; Tao, N. J. Large Gate Current Modulation in a Room Temperature Single Molecule Transistor. *J. Am. Chem. Soc.* **2005**, *127*, 2386–2387.
31. Li, X.; Hihath, J.; Chen, F.; Masuda, T.; Zang, L.; Tao, N. J. Thermally Activated Electron Transport in Single Redox Molecules. *J. Am. Chem. Soc.* **2007**, *129*, 11535–11542.
32. Su, W.; Jiang, J.; Lu, W.; Luo, Y. First-Principles Study of Electrochemical Gate-Controlled Conductance in Molecular Junctions. *Nano Lett.* **2006**, *6*, 2091–2094.
33. Zhang, J.; Kuznetsov, A. M.; Ulstrup, J. *In Situ* Scanning Tunnelling Microscopy of Redox Molecules. Coherent Electron Transfer at Large Bias Voltages. *J. Electroanal. Chem.* **2003**, *541*, 133–146.
34. Zhang, J.; Chi, Q.; Kuznetsov, A. M.; Hansen, A. G.; Wackerbarth, H.; Christensen, H. E. M.; Andersen, J. E. T.; Ulstrup, J. Electronic Properties of Functional Biomolecules at Metal/Aqueous Solution Interfaces. *J. Phys. Chem. B* **2002**, *106*, 1132–1152.
35. Zhang, J.; Kuznetsov, A. M.; Medvedev, I. G.; Chi, Q.; Albrecht, T.; Jensen, P. S.; Ulstrup, J. Single-Molecule Electron Transfer in Electrochemical Environments. *Chem. Rev.* **2008**, *108*, 2737–2791.
36. Tao, N. J. Probing Potential-Tuned Resonant Tunneling through Redox Molecules with Scanning Tunneling Microscopy. *Phys. Rev. Lett.* **1996**, *76*, 4066–4069.
37. Pobelov, I. V.; Li, Z.; Wandlowski, T. Electrolyte Gating in Redox-Active Tunneling Junctions−An Electrochemical STM Approach. *J. Am. Chem. Soc.* **2008**, *130*, 16045–16054.
38. Artés, J. M.; Díez-Pérez, I.; Gorostiza, P. Transistor-like Behavior of Single Metalloprotein Junctions. *Nano Lett.* **2011**, 10.1021/nl2028969.
39. Alessandrini, A.; Gerunda, M.; Canters, G. W.; Verbeet, M. Ph.; Facci, P. Electron Tunnelling through Azurin is Mediated by the Active Site Cu Ion. *Chem. Phys. Lett.* **2003**, *376*, 625–630.
40. Kuznetsov, A. M.; Ulstrup, J. Mechanisms of *in Situ* Scanning Tunneling Microscopy of Organized Redox Molecular Assemblies. *J. Phys. Chem. A* **2000**, *104*, 11531–11540.
41. Marcus, R. A. On the Theory of Oxidation-Reduction Reactions Involving Electron Transfer. *J. Chem. Phys.* **1956**, *24*, 966–978.
42. Iversen, G.; Kharkats, Y. I.; Kuznetsov, A. M.; Ulstrup, J. Electron Transfer: From Isolated Molecules to Biomolecules. In *Advances in Chemical Physics*; Jortner, J., Bixon, M., Eds.; Wiley: New York, USA, 1999; Vol. 106, pp 453−514.